Control of an AUV with Saturating Actuators: Classical and LMI based Design Approaches

Jean-Pierre Folcher and Abel Piña
Laboratoire d'Informatique, Signaux et Systèmes de Sophia Antipolis (I3S)
2000 route des Lucioles, BP 121, 06509 Sophia Antipolis Cedex, France
folcher@i3s.unice.fr

***Abstract*-The problem of designing the diving controller for the autonomous underwater vehicle MAUVE is discussed in this paper. To reflect all the control features and specifically the actuator saturation, a LMI-based controller design with input saturation is presented. Then, a structured controller (pitch and depth control loops) is designed using a heuristic based on classical methods which explicitly takes into account the saturation constraint. Finally, the convex synthesis method is applied to design the diving controller. Numerical simulations show that the LMI controller presents some advantages.**

I. INTRODUCTION

Guidance and control systems for autonomous underwater vehicles (AUV) are developed separately : control systems are designed based on vehicle dynamics whereas guidance laws are based on kinematic relationships. During the design phase, a pragmatic approach consists in designing the control system with sufficiently large bandwidth to track the commands that are expected from the guidance system (the so called time-scale separation principle). This approach generates high gain control loops and high level peak command inputs. If the actuator saturation level is not taken into account explicitly, stability and performance of the closed loop systems are not guaranteed. This potential problem is particularly serious in the case of severe operating conditions of underwater vehicles: high maneuvering trajectories, precision station keeping, strong current disturbances. In this context, tight restrictions on the closed loop bandwidth (which may lead to actuator saturations) are expected.

A classical approach to deal with this specific problem is the anti wind-up design [1], [2]. A controller is first designed ignoring the input saturations. Then, it is modified to take into account the effects of non linearities. The last step is the verification of the stability and the performance of the closed loop system. It is thus a *``trial and error''* approach. The purpose of this paper is to propose a design method which avoids this *``trial and error''* procedure, by avoiding actuator saturations. It is a modification of previously published results, see [3], which allows to design a low complexity output feedback control law using a low complexity design methodology, and ensuring a certain level of performance in terms of stability and L_2 gain. The numerical resolution reduces to a finite dimensional, convex optimization problem including Linear Matrix Inequalities (LMI) constraints. This control methodology is applied to the control of the diving motion of the MAUVE underwater vehicle. The difficulty of the problem is reinforced by tight performance requirements as well as the presence of low actuator saturation levels that limit the control bandwidth.

The paper is organized as follows. Section II. is dedicated to the presentation of the MAUVE diving motion control problem. In section III., the controller design method is presented. Pitch and depth controllers are designed in section IV. using both classical design tools and the proposed design method. Numerical experiments allow us to compare the two designs. Some concluding remarks and perspectives end the paper in section V.

II. MAUVE VEHICLE CONTROL PROBLEM

A. MAUVE Vehicle

Mauve is an autonomous underwater vehicle dedicated to measurements of oceanographic parameters in coastal areas. It is a small and light vehicle with a torpedo (cylindrical) shape, with all the propulsion at the rear. Its motion in the 3D space is controlled by two fins: one for diving motion and another for heading motion. The maximum depth of operation is 70 meters and its endurance is about 2 hours at 4 knots. Its main characteristics are:

- its small size (1,9 m length, diameter 0.15 m.) and weight (30 Kg in the air), making it easily operated by a single person from a small boat,
- its reconfiguration capability, the user payload is modular and can accommodate a wide variety of sensors,
- an user-friendly interface for mission definition and data upload is an integral part of the system.

In the context of the SUMARE (SUrvey of MArine Resources) research project, the underwater autonomous vehicle MAUVE will be used to produce bathymetric observations of the Kwintebank, in the coast of Belgium. The vehicle will be used in two distinct navigation modes: performing a set of straight lines (tracks) in a direction transversal to the sand bank and tracking lines of constant depth of the sea floor. This specific navigation scenario presents several difficulties: the low depths attained in some parts of the bank (which can be as low as 5 meters), and the strong currents (up to 4 knots) impose that the vehicle's trajectory be very stable and a high gain control policy. These two controls objectives are conflicting. The control method presented in the following section is well suited to obtain the best performance trade-off for the vertical control system which is the main component of this specific navigation problem.

Fig.1. Launching MAUVE.

B. MAUVE Vertical Control Problem

The MAUVE vehicle motion is described a differential equation in six degrees of freedom which can be divided into three non interacting or lightly interacting subsystems: surge dynamics, steering dynamics and diving dynamics. In this context, the control system design can be cast as three separate designs for the forward speed controller, the steering controller and the diving controller. This control philosophy is a current practice for underwater robots. This section is concerned with the combined pitch and depth (diving) control of MAUVE, represented schematically in Fig.2.

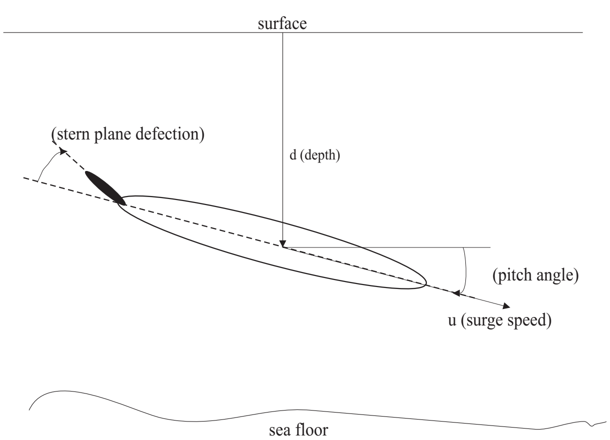

Fig. 2. MAUVE motion in the vertical plane.

The pitch angle θ represents the angle between the horizontal plane (defined by the sea surface) and the longitudinal axis of the vehicle. This angle is measured by an inclinometer. A pressure sensor evaluates the depth d. The vertical motion is controlled by the deflection of the stern plane δ_θ, which is actuated by a servomotor. The diving controller objectives are to ensure stability and tracking properties for the vehicle trajectory defined by the higher level control.

From the control point of view, the flight of Mauve can be divided into two main periods:

- *the descent phase*: up on launching, the robot has to attain a required mission depth. The diving controller has to ensure a specified pitch descent angle for a nominal surge speed u_0 of 2m/s. During this period, the diving controller objective is to track the given pitch reference.
- *the navigation phase*: when the mission depth is attained, the navigation phase starts and the control objective is to maintain the specified reference depth.

C. Control Strategy and Specifications

The choice of a combined structure (inner pitch control loop and a outer depth control loop) allows:

- to take into account clearly the different control objectives during the descent and the navigation phases,
- to keep a strong physical interpretation of the control policy and, consequently, to facilitate the design and the validation of the diving controller.

The block diagram of a linearized model of the plant (actuator, robot mechanics, pitch and depth sensors) in loop with this structured linear controller is depicted on the next figures.

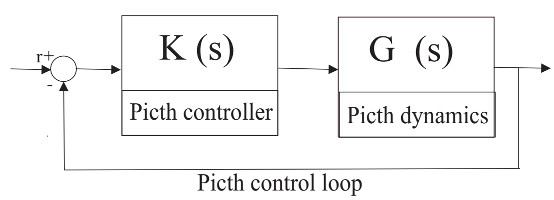

Fig. 3. closed loop system during the descent phase.

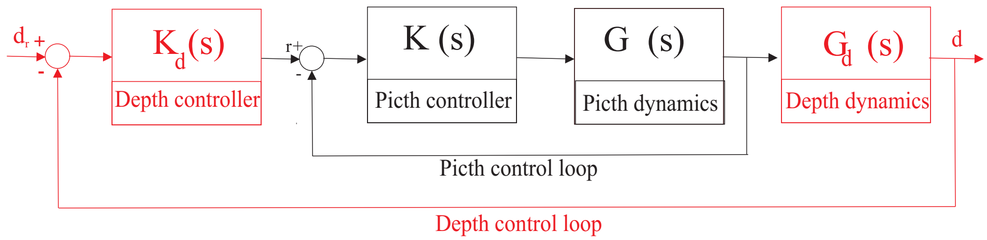

Fig. 4. closed loop system during the navigation phase.

Diving closed loop specifications.

(i) The settling time (5 %) is minimized and the overshoot is acceptable (on the order of 5%).

(ii) The steady state error for a reference step is about zero.

(iii) For a 5 meter step input, the controller output (stern deflection) is limited in magnitude to 17.

D. Vertical Dynamic Model

The transfer function $G_{\theta\delta_\theta}(p)$ describes the relation between stern plane defection δ_θ and measured pitch angle θ. The dynamic dependence between the depth d and the pitch angle θ is governed by the transfer function $G_{d\theta}(s)$. Under simplifying assumptions (neglecting sway, yaw and heave velocities) verified in nominal operating conditions, the transfer functions above can be written as, see [4] :

$$G_{\theta\delta_\theta}(s) = \frac{\theta(s)}{\delta_\theta(s)} = \frac{b_0}{s^2 + a_1 s + a_2},$$

and

$$G_{d\theta}(s) = \frac{d(s)}{\theta(s)} = \frac{-u_0}{s}.$$

From signals recorded at sea and standard identification techniques (least squares method, maximum likelihood estimation), see for instance [5], we obtain the following model parameters

$$\begin{pmatrix} b_0 \\ a_1 \\ a_2 \\ u_0 \end{pmatrix} = \begin{pmatrix} 0.0806 \\ 0.4739 \\ 0.0276 \\ 2{,}2563 \end{pmatrix}.$$

III. LMI BASED DESIGN METHOD

In this section, main results about the design approach based on Lyapunov approach combined with Linear Matrix Inequality (LMI) optimization in the spirit of [6] are presented. For a more detailed presentation and complete proofs we refer the reader to [7].

A. Problem Statement

We consider the linear time invariant system described by the following state space equations

$$\begin{aligned} \dot{x} &= Ax + B_w w + B_u u, \\ z &= C_z x + D_{zw} w + D_{zu} u, \\ y &= C_y x + D_{yw} w, \end{aligned}$$

where $x : R^+ \to R^n$ is the state, $w : R^+ \to R^{n_w}$ is the exogenous output , $u : R^+ \to R^{n_u}$ is the command input, $z : R^+ \to R^{n_z}$ is the regulated output, and $y : R^+ \to R^{n_y}$ is the measured output.

B. Control Objectives

The purpose is to find a strictly proper LTI controller in closed loop with the system which achieves simultaneously a number of desired properties. The closed-loop system is represented on Fig. 5.

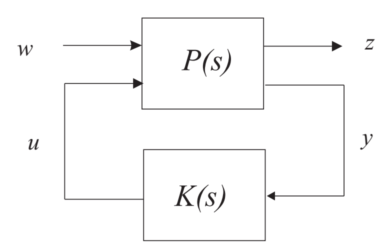

Fig. 5. Standard control problem.

Consider a polytope P of initial conditions containing the origin, described by its vertices $P = Co\{v_1, \ldots, v_p\}$, where Co denotes the convex hull. Furthermore, assume that the disturbance input has an L_2 norm less than one, that is, for every $T > 0$

$$\int_0^T w(t)^T w(t) dt \le 1 .$$

This expression can be interpreted as a bound over the energy of the input w. The closed loop system must have the following performance properties.

S.1 ***Stability.*** For all disturbance input w unitary and for all initial condition $x(0) \in P$, the closed loop system is stable.

S.2 ***"Weak" L_2 -gain***. For every $T > 0$, the disturbance input w and the regulated output z satisfy

$$\int_0^T z(t)^T z(t) dt < \gamma^2 \int_0^T w(t)^T w(t) dt + \beta(x(0)) .$$

S.3 ***Input peak bound.*** For all trajectories defined in **S.1** each ith coordinate of u satisfy, for some prespecified number u_{sat}

$$|u_i(t)| \le u_{sat} \quad \text{for every } t \ge 0 .$$

C. Synthesis Conditions

The synthesis conditions given in this paragraph are those exposed in [7] for *non-saturating controller.*

Theorem. *If there exist symmetric matrices* $P, Q \in R^{n \times n}$, and matrices $Y = \begin{pmatrix} Y_1^T & \cdots & Y_{n_u}^T \end{pmatrix}^T \in R^{n_u \times n}$ and $Z \in R^{n \times n_y}$ such that

$$\begin{bmatrix} A^T P + PA + C_z^T C_z + C_y^T Z^T + Z C_y & PB_w + C_z^T D_{zw} + Z D_{yw} \\ B_w^T P + D_{zw}^T C_z + D_{yw}^T Z^T & D_{zw}^T D_{zw} - \gamma^2 I \end{bmatrix} < 0,$$

$$\begin{bmatrix} AQ + QA^T + B_u Y + Y^T B_u^T + B_w B_w^T & QC_z^T + Y^T D_{zu}^T + B_w D_{zw}^T \\ C_z Q + D_{zu} Y + D_{zw} B_w^T & D_{zw}^T D_{zw} - \gamma^2 I \end{bmatrix} < 0,$$

$$v_j^T P v_j \le \beta \quad , \quad for \quad j = 1, \ldots, r ,$$

$$u_{sat} \begin{bmatrix} \frac{\gamma^2}{\gamma^2 + \beta} I & 0 & 0 \\ 0 & Q & \gamma I \\ 0 & \gamma I & P \end{bmatrix} + \begin{bmatrix} 0 & Y_i & 0 \\ Y_i^T & 0 & 0 \\ 0 & 0 & 0 \end{bmatrix} \ge 0, i = 1, \ldots, n_u$$

then, there exists a strictly proper full order output feedback controller with state space matrices

$$\bar{A} = M^{-1} \cdot \Bigg(PA + \gamma^2 A^T Q^{-1} + PB_u Y Q^{-1} + Z C_y - \begin{bmatrix} (PB_w + Z D_{yw})^T \\ C_z \end{bmatrix}^T \begin{bmatrix} -\gamma^{2I} & D_{zwzw}^T \\ D_{zw} & -I \end{bmatrix}^{-1} \begin{bmatrix} \gamma^2 B_w^T Q^{-1} \\ C_z + D_{zu} Y Q^{-1} \end{bmatrix} \Bigg) M^{-1},$$

$$\bar{B} = M^{-1} Z,$$

$$\bar{C} = -Y Q^{-1} M^{-1}, \; where \;\; M^2 = P - \gamma^2 Q^{-1} ,$$

in closed-loop with the system which ensures the control objectives **S.1**, **S.2** *and* **S.3.**

IV. DIVING CONTROLLER DESIGN

A. Pitch/Depth Controller Classical Design

An underlying assumption when designing separately the pitch and depth controllers is the pitch loop has a sufficiently large bandwidth to track the command that are generated by the depth controller (the so called *time-scale separation principle*). In this context, the pitch closed loop system is represented on Fig. 3. A simplified block diagram for the depth controller design is given on Fig 6.

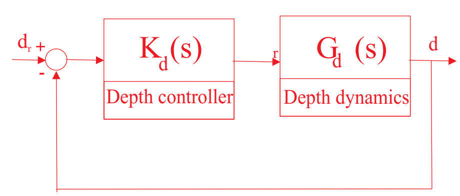

Fig. 6. simplified depth control loop.

The time-scale separation principle is not valid under saturation phenomena. In fact, imposing outer loop slow dynamics when compared to the inner loop (fast) dynamics, and guaranteeing that the actuator never saturates are conflicting objectives. In the sequel, we present a method which explicitly takes into account the saturation phenomena acting on the fins. Consider the simplified depth closed loop depicted on Fig.6 where the controller has a proportional integral (PI) structure

$$K_c^d(s) = k^d\left(1 + \frac{1}{T_I^d}\right).$$

For a reference input step of given size Δ_d, and for a fixed value of the settling time t_s^d we can obtain controller parameters k^d, T_I^d using a classic design method (root locus, frequency method). The maximum value of the controller output, $\theta_{\max}$, defined as

$$\theta_{\max} = \max_{t \geq 0}\left(\left|\theta\ (t)\right|\right)$$

can be compute using temporal simulations. We have an implicit relation between the controller parameters k^d, T_I^d, the step size Δ_d, the settling time t_s^d, and the maximum value of the controller output $\theta_{\max}$. For the given fixed size step specified in II.C., $\Delta_d = 5m$, the trade-off curve of $\theta_{\max}$ versus the settling time t_r^d is plotted on Fig. 7.a. Remark that a small depth settling time t_r^d corresponds to a high value of $\theta_{\max}$.

A similar reasoning can be applied for the pitch control loop by considering also a PI controller. In this case, we consider a fixed value for $\delta_{\theta_{\max}} = \max_{t \geq 0}\left(\left|\delta_\theta(t)\right|\right)$ $= \delta_{\theta_{sat}} = 17$, according to the specification in II.C. The step size Δ_{δ_θ} is plotted on Fig. 7.b.versus the settling time t_s^θ. Note that for decreasing values of t_s^θ, the step size Δ_{θ_r} is decreasing. The key point consists in tuning t_r^d and t_s^θ such that $\theta_{\max} = \Delta_{\theta_r}$.

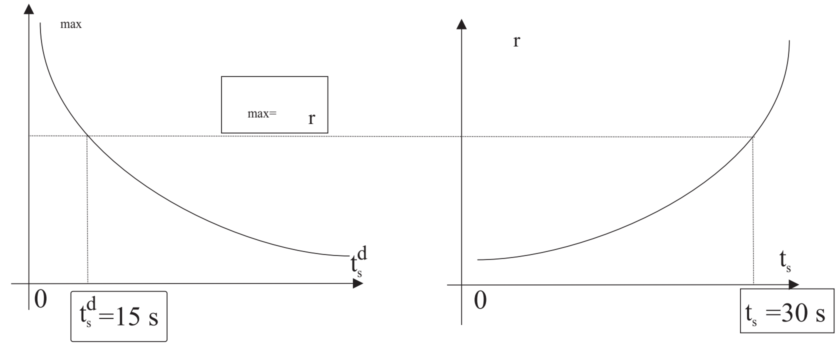

(a) pitch loop trade-off.

(b) depth loop trade-off.

Fig. 7. Classical design trade-off curves.

The results are the following

$$t_r^d = 30s, t_r^\theta = 15s.$$

Using the root locus method, we obtain for the specified settling time $t_r^\theta = 15s$ the following controller transfer function

$$K_\theta^c(s) = 0.114\frac{1+9s}{s}.$$

The time-scale separation principle is violated and to achieve the depth controller design, the complete closed loop pitch dynamics must be described by the following transfer function

$$G_{depth}(s) = \frac{K_\theta(s) \cdot G_{\theta\delta\theta}(s)}{1 + K_\theta(s) \cdot G_{\theta\delta\theta}(s)} G_{d\theta}(s).$$

Using a frequency design method, the depth controller transfer function ensuring a phase margin $PM = 50°$ and a cut-off frequency of $0.413\ rd/s$ is determined:

$$K_d^c(s) = 2.55\frac{10s+1}{10s}.$$

B. Pitch Controller LMI Design

The LMI specification **S.2** imposes a H_∞-norm performance between input w and output z. This feature allows to build a loop shaping method and to express performance as frequency constraints see [8]. The pitch closed loop system is represented on the loop shaping synthesis block diagram

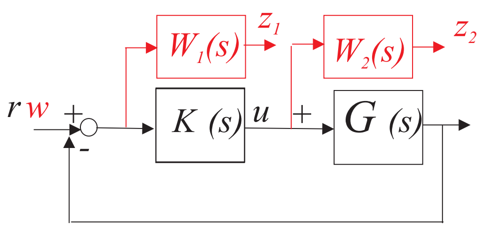

Fig. 8. Loop shaping control problem.

If **S.2**. is ensured with $\gamma = 1$, then the transfer function between input w and output z has the property

$$\left\| T_{zw}(s) \right\|_\infty = \left\| \begin{matrix} T_{z_1 w_1}(s) \\ T_{z_2 w_2}(s) \end{matrix} \right\|_\infty = \left\| \begin{matrix} T_{\varepsilon\theta_r}(s) W_1(s) \\ T_{u\theta_r}(s) W_2(s) \end{matrix} \right\|_\infty \leq 1,$$

and consequently

$$\left| T_{\varepsilon\theta_r}(j\omega) \right| < \frac{1}{\left| W_1(j\omega) \right|} \text{ and } \left| T_{u\theta_r}(j\omega) \right| < \frac{1}{\left| W_2(j\omega) \right|}.$$

The procedure to choose the weighting functions $W_1(s)$, $W_2(s)$ is explained in [8]. We fix

$$W_1(s) = \frac{1}{2} \frac{(s+0.2)^2}{(s+2\,10^{-4})^2} \text{ and } W_2(s) = 10 \frac{s+10}{s+1000}.$$

For the LMI design we have chosen

$$P = Co\left\{ (0 \quad 2.8)^T \right\},\ (\gamma, \beta) = (0.9001, 2000),\ u_{sat} = 17.$$

The LMI optimization problem was solved using the the commercial Matlab toolbox *LMI Control Toolbox* [9] . The state space representation of the pitch controller is

$$\bar{A} = \begin{bmatrix} -4.20 & -31.14 & 0 & 0.01 \\ 0.30 & 1.58 & 0 & 0 \\ 0 & 0 & 0 & 0 \\ 0 & 0 & 0 & 0 \end{bmatrix} \bar{B} = \begin{bmatrix} 0.09 \\ 1.06 \\ -16143 \\ -25177 \end{bmatrix}, \bar{C} = \begin{bmatrix} 0.14 \\ 1.44 \\ 0 \\ 0 \end{bmatrix}^T.$$

We can check on Fig. 9. and Fig.10 that the frequency specifications are met for both transfer functions $T_{\varepsilon\theta_r}(s)$ and $T_{u\theta_r}(s)$. The step responses of the system in loop with the ''classical'' controller and with the LMI controller are plotted for the command input on Fig.11. and for the measured output on Fig. 12. For figures 9 to 12, dashed lines are responses of the ''classical'' controller, while plain lines represent the LMI controller responses.

Remark that the LMI controller ensures a better settling time. It guarantees also that for a specified set of initial conditions the controller never saturates. Note that this control objective is not explicitly taken into account with the classical design method.

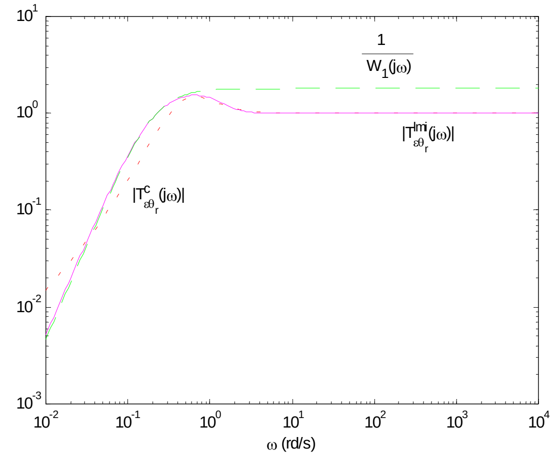

Fig. 9. $T_{\varepsilon\theta_r}(s)$ Bode diagram.

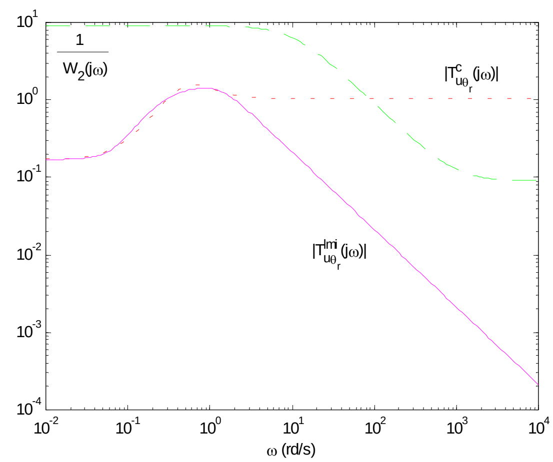

Fig. 10. $T_{\delta\theta_r}(s)$ Bode diagram.

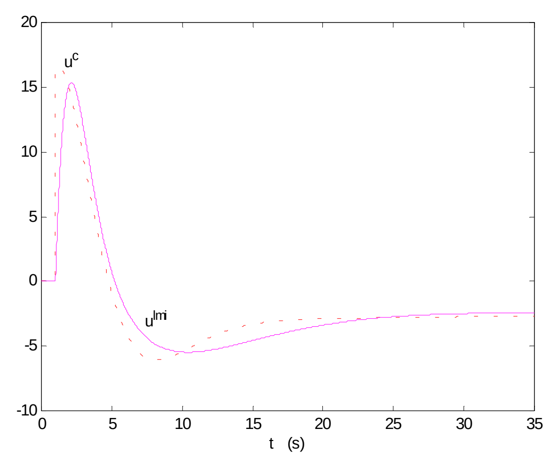

Fig. 11. Command u time response for a 16° step input θ_r .

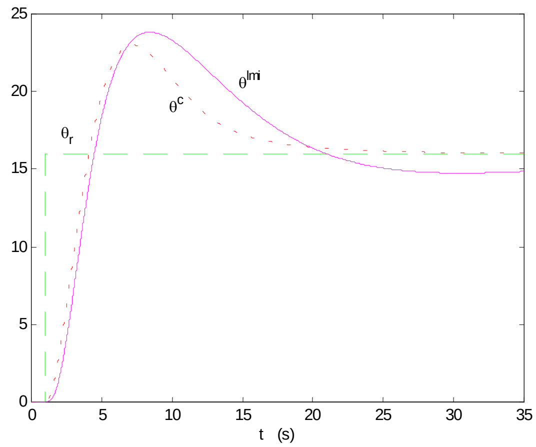

Fig. 12. Pitch θ time response for a 16° step input θ_r .

C. Depth Controller LMI Design

We consider basically the same standard synthesis problem for the complete closed loop pitch dynamics described by the following transfer function

$$G_d^{lmi}(s)=\frac{K_\theta(s)\cdot G_{\theta\delta\theta}(s)}{1+K_\theta(s)\cdot G_{\theta\delta\theta}(s)}G_{d\theta}(s) .$$

In this context, specification **S.3** is associated to the controller output θ_r . The saturation phenomena concerns the internal signal δ_{θ_r} of the pitch loop. We compute a state space representation for this system with new output δ_θ as

$$\begin{aligned}
\dot{x} &= Ax+B_w w+B_u u,\\
z &= C_z x+D_{zw}w+D_{zu}u,\\
\delta_\theta &= C_{\delta\theta}x,\\
y &= C_y x+D_{yw}w.
\end{aligned}$$

The fourth LMI of the theorem in section III is rewritten as

$$C_{\delta\theta}QC_{\delta\theta}^T \le \frac{\gamma^2}{\gamma^2+\beta}u_{sat}^2 .$$

Unfortunately, numerical problems lead to baddly conditioned controller state space representation. We relax the design problem to take into account only H_∞-norm loop shaping constraint. This synthesis method gives the following depth controller

$$\overline{A}=\begin{pmatrix}
-0.002 & 0 & 0 & 0 & 0 & 0\\
-8.213 & -2.648 & -3.657 & -1.108 & -1.380 & -0.464\\
0 & 0 & 0 & 0 & 0.25 & 0\\
-0.143 & 1.697 & -0.063 & -0.999 & -0.482 & 0.235\\
0 & 0 & 0 & 1 & 0 & 0\\
-0.065 & 0.773 & -0.029 & -0.008 & -0.260 & -0.003
\end{pmatrix},$$

$$\overline{B}=\begin{bmatrix}1.118\\0\\0\\0\\0\\-0.003\end{bmatrix},\quad \overline{C}=\begin{bmatrix}-0.082\\0.978\\-0.036\\-0.011\\-0.013\\-0.004\end{bmatrix}^T$$

We can check that the frequency performance specifications are ensured on Fig.13. and Fig.14. Again, the closed loop transfer functions associated to the ‘’classical’’ controller are plotted in dashed line and the closed loop transfer functions associated to the ‘’LMI’’ controller are depicted in plain line.

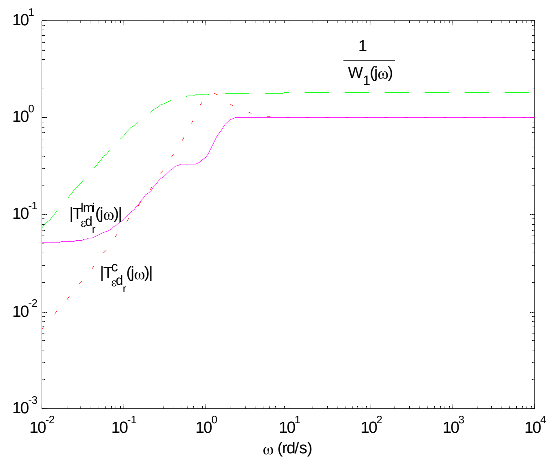

Fig. 13. $T_{\varepsilon d_r}(s)$ Bode diagram.

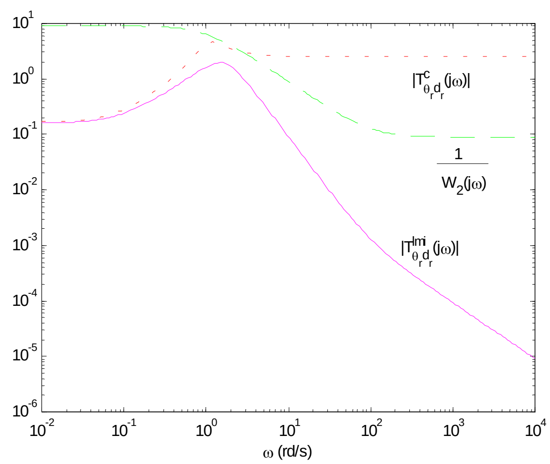

Fig. 14. $T_{\theta_r d}(s)$ Bode diagram.

For a 16°.step input reference, the following closed loop system responses have been obtained. The ''classical'' depth controller response is plotted in dashed line while the LMI depth controller response is depicted in plain line.

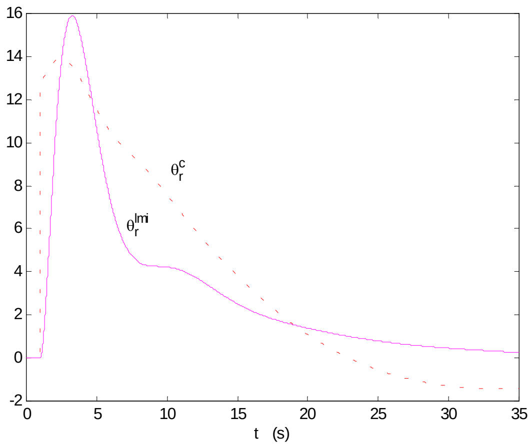

Fig. 15. command input u time response

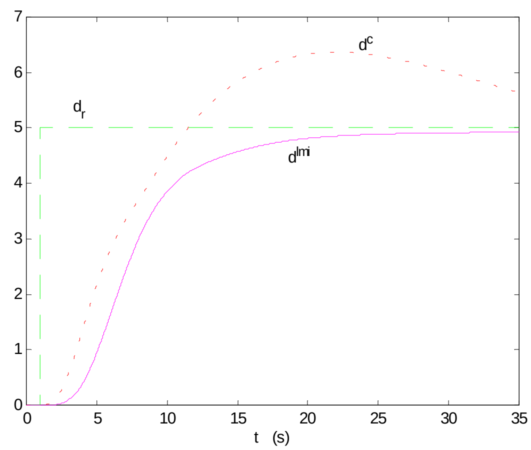

Fig. 16. Pitch θ time response

Note that the command input does not excite the saturation for the two closed loop systems. The system in loop with the LMI controller ensures better performance in terms of settling time which is about 15s.

V. CONCLUSIONS AND PERSPECTIVES

In this paper, we presented a control method for autonomous underwater vehicles with saturating actuators. This approach is based on the design of an output feedback controller involving LMI optimization problem. Practical specifications are ensured by shaping main closed loop transfer functions. The approach ensures also local stabilization for a specified set of initial conditions and under a set of disturbance inputs. In our opinion, this approach directly uses control engineering expertise and allows to obtain a clear trade-off between performance and saturation constraint. Finally, the method is applied to the design of the diving controller of the underwater vehicle MAUVE. The achieved performances have been compared to a structured PI controller designed earlier. The LMI diving controller gives satisfactory results. The proposed control method guarantees that the obtained controller has a control magnitude bounded by a given level. This controller is referred to as a *non-saturating controller*. If we allow command input higher than the saturation level, a portion of the saturation is "excited" and this information can be used to guarantee absolute stability of the "excited" nonlinearity. This controller is referred to a *saturating controller* and has a Linear Time Varying (LTV) structure. Synthesis conditions can be cast as an LMI optimization problem, see [7]. Future work will include:

– design of saturating controller for the MAUVE vertical motion,
– design of the steering controller and the propeller controller,
– extensive sea testing showing the robust performance.

Acknowledgments

This work has been partially funded by the European Union trough research contracts SUMARE (IST-1999-10836, Survey of Marine Resources).

REFERENCES

[1] A. H. Glattfelder and W. Schaufelberger, "Stability Analysis of Single Loop Control Systems with saturation and Antireset-windup circuits", *IEEE Transactions on Automatic Control,* Vol. 28, No. 12, 1074-1081, 1983.

[2] M.V. Kothare M.V., P.J. Campo, M. Morari, and C.C. Nett. "A unified framework for the study of anti-windup Reset," *European Journal of Control,* vol. 7, pp. 567-579, 2001.

[3] L. El Ghaoui and J.P. Folcher. "Multiobjective robust control of system subject to unstructured perturbations," *Systems & Control Letters,* vol. 7, n. 1, pp. 23-30, 1996.

[4] T.I. Fossen, *Guidance and control of ocean vehicles*. John Wiley & Sons, 1995.

[5] J.-P. Folcher, and J. Rendas, "Identification and control of the Phantom 500 body motion,'' Proceedings of Oceans'01, Hawaï, 2001.

[6] S. Boyd, L El Ghaoui, E. Feron, and V. Balakrishnan, *Linear matrix inequalities in systems and control theory,* volume 15 of Studies in Applied Mathematics, SIAM, Philadelphia, PA, June 1994.

[7] G. Scorletti, J.P. Folcher, and L. El Ghaoui, "Output feedback control systems with input saturations: LMI design approaches," *Automatica,* Vol. 30, No. 12, 1869-1883, *1994* .

[8] J.-P. Folcher,, "Robust design framework for an underwater vehicle motion Controller,'' Proceedings of Oceans'02, to appear.

[9] P. Gahinet, A. Nemirovsky, A. L. Laub, and M. Chilali, *LMI control toolbox*, The Mathworks Inc., 1995.